

# Plasma Polymerization of Tetrafluoroethylene. I. Inductive Radio Frequency Discharge

H. YASUDA\* and N. MOROSOFF, *Research Triangle Institute, Research Triangle Park, North Carolina 27709*, and E. S. BRANDT and C. N. REILLEY, *Department of Chemistry, University of North Carolina, Chapel Hill, North Carolina 27514*

## Synopsis

The plasma polymerization of tetrafluoroethylene in an inductively coupled radio frequency glow discharge, using a flow system, was studied. A simple long tube reactor, with the coupling coil placed at the middle of the tube and gas entrance and exit at the respective ends, was used. Deposition rates and the chemical nature of the polymer (as revealed by ESCA spectra and surface energy studies) are obtained as a function of location in the reactor tube with respect to the coupling coil and of applied energy per unit mass of tetrafluoroethylene ( $W/FM$ ). It was found that a fluorine-poor polymer, containing considerable carbon-oxygen bonds (after contact with air), is obtained at all locations at high  $W/FM$ . When a low  $W/FM$  is utilized, such a fluorine-poor polymer is also obtained at locations downstream from the coupling coil (the location of the highest energy density) in the reactor. In the latter case a fluorine-rich polymer containing very little oxygen is formed upstream from the coil. The polymer deposition rate distribution is also considerably broader in a high  $W/FM$  plasma than when low  $W/FM$  is used. These results are in agreement with earlier studies indicating that fluorine abstraction and decomposition due to fluorine etching occur when the energy density, as expressed by  $W/FM$ , is high.

## INTRODUCTION

The most important feature of plasma polymerization is that ultrathin layers of highly crosslinked polymer network which adhere tenaciously to an organic polymer substrate can be obtained directly from the vapor of the monomer by a relatively simple process of electric discharge. On the other hand, the actual chemical reactions involved in this simple operation are extremely complex, and the advantageous features mentioned above become serious drawbacks in an effort to elucidate chemical reactions involved and/or properties of polymers formed. The highly crosslinked and grafted layer hampers the conventional analysis of polymers, such as the determination of molecular weight (and its distribution) and structural analysis which can be applied to a solution of polymer. Therefore, the basic study of plasma polymerization is extremely difficult and the understanding of the process lags far behind the technical exploitation of the process.

Data obtained by analysis of gas phases, such as by mass spectrometry<sup>1-10</sup> and by emission spectroscopy<sup>11</sup> measurements, and the analysis of polymers that are soluble in solvents<sup>11,12</sup> provide important information. However, this is not direct information on polymers resulting from plasma polymerization that have the unique characteristics and advantages described above.

\*Present address: Department of Chemical Engineering, University of Missouri, Rolla, MO 25401.

The use of ESCA (electron spectroscopy for chemical analysis) has a special appeal in the study of plasma polymerization, because the analysis is based on the surface (to a depth of less than 50 Å) and is not hampered by the properties of the substrate. On the other hand, due to typically small binding energy changes (i.e., chemical shifts) of organic elements, ESCA is primarily used for elemental analysis of the surface. The structural analysis of organic compounds by ESCA is limited to some special cases where large chemical shifts can be observed (i.e., typically  $>2$  eV). Consequently, for the study of plasma polymerization of hydrocarbons, for instance, ESCA provides rather limited information since the chemical shift in the binding energy of carbon due to various chemical structures in such a polymer, where carbon is bound primarily to other carbons and hydrogens, is typically too small to be detected in a quantitative manner.

However, the use of perfluorocarbons as monomers for plasma polymerization provides an interesting model study because fluorine causes a large (ca. 2–3 eV per fluorine atom) chemical shift in the binding energy of carbon. The study of plasma polymerization of tetrafluoroethylene by ESCA has pointed out important aspects of plasma polymerization which were not obvious in plasma polymerization of hydrocarbons. This point can be further elaborated by an example of plasma polymerization of tetrafluoroethylene.

When polytetrafluoroethylene is formed from monomer tetrafluoroethylene by a conventional method, all carbons excluding terminal groups in the polymer contain two fluorine atoms. Consequently, the ESCA C1s peak of polytetrafluoroethylene (e.g., Teflon TFE) is a singlet at about 292 eV. However, a typical plasma polymer of tetrafluoroethylene generally contains C1s peaks corresponding to  $\text{CF}_3$ ,  $\text{CF}_2$ ,  $\text{CF}$ , and hydrocarbon carbon (not attached to F).

It is also observed that under certain conditions a plasma polymer of tetrafluoroethylene similar to Teflon TFE can be obtained.<sup>14</sup> This implies that considerable rearrangement of monomer structure, perhaps due to fragmentation and recombination, occurs during the process of forming a polymer in plasma. This kind of rearrangement would also occur in plasma polymerization of hydrocarbons; however, no tool is currently sensitive enough to investigate the effects directly.

Thus, tetrafluoroethylene, or perfluoro carbons in general, provide an ideal case for ESCA polymer studies because the structural aspects of polymer and the polymerization mechanisms which lead to such structure can be investigated by this technique as functions of experimental parameters. Therefore, in this study tetrafluoroethylene was chosen as a monomer for plasma polymerization in order to investigate the effects of various experimental factors, such as flow rate, discharge power, etc.

Using a simple straight-tube reactor, the properties of polymer are investigated as a function of location within a tube. In such a reactor, glow extends in the upstream side of the rf coil nearly as far as in the downstream side. Therefore, it provides an interesting case for studying the interrelationship of monomer flow, transport of excitation, and polymer formation.

## EXPERIMENTAL

The reaction tube used in this study is a straight Pyrex glass tubing (O.D. 16 mm and length approximately 100 cm) with a standard tapered glass joint at each end by which the reactor is connected to a vacuum system which has been de-

scribed in previous studies. The rf coil is located in the center of the reaction tube, and the monomer is introduced into one end of the tube and pumped out from the other end. The location of the center of the rf coil is taken as the zero point, and the distance from the zero point is measured in the direction of flow.

Polymer is collected onto  $1 \times 2$  cm aluminum foils which are placed inside a glass tube (O.D. 11 mm and length approximately 5 cm). The inner glass tubes (with and without aluminum foil) are inserted into a reaction tube so that aluminum foils will be located at the designated positions.

Based on results of a previous study,<sup>13</sup> two levels of energy input, i.e.,  $1.9 \times 10^7$  and  $7.7 \times 10^8$  J/kg monomer, were employed. The energy input level (in joules per kg of monomer, J/kg) is given by  $(W/FM) \times 1.34 \times 10^9$ , where  $W$  is discharge power in watts,  $F$  is flow rate in  $\text{cm}^3$  (S.T.P.)/min, and  $M$  is molecular weight in grams.<sup>15</sup>

At the lower level of energy input, the plasma glow covers only a part of the reactor tube, and two aluminum foils in the downstream side are located in the nonglow region. Glow in the upstream side of the rf coil extended just beyond the foil located at the  $-18$  cm position. At the higher level of energy input, glow covers the entire length of the reaction tube.

The weight increases of the aluminum foils were measured by a Cahn electrobalance to calculate the deposition rate at each location.

ESCA spectra were obtained by using a du Pont Model 650 spectrometer with a  $\text{MgK}\alpha$  x-ray source and equipped with a microcomputer data acquisition and processing system. The details of experimental procedures were described in a previous paper.<sup>16</sup>

Surface energy analyses were carried out by measuring contact angles of various liquids of known surface energy components, and the dispersive force component  $\gamma_d$  and polar component  $\gamma_p$  were calculated according to the methods described by Kaeble.<sup>17</sup>

## RESULTS AND DISCUSSION

The deposition rate observed in the glow region of the rf discharge is proportional to the flow rate of the monomer. Therefore, in order to compare the polymerization characteristics in two conditions used in this study, the deposition rate/flow rate [D.R./F] is shown as a function of the location of polymer deposition in Figure 1. The center of the rf coil is taken as the zero point, and the distance in the direction of the monomer flow is used to express the location of polymer deposition. The extent of glow is shown by the shaded band; i.e., in the case of  $1.9 \times 10^7$  J/kg, the glow covers the range of approximately  $-18$  to  $18$ , whereas in the case of  $7.7 \times 10^8$  J/kg, the glow covers the entire reaction tube. As seen in Figure 1, in the case of low energy input, polymer tends to deposit in the vicinity of the rf coil; but at the higher energy input, polymer deposits in the entire reaction tube in a more even manner. It is interesting to note that the integrated areas for both cases are nearly identical, indicating that the total polymer formed per unit flow is essentially the same.

The ESCA spectrum was taken for samples of plasma polymer deposited on aluminum substrates for 1.5 min. The results are summarized in Table I. The spectrum of conventionally prepared Teflon shows a single intense peak at about 292 eV corresponding to the  $-\text{CF}_2-$  carbon species.  $\text{CF}_3$ -type carbons would

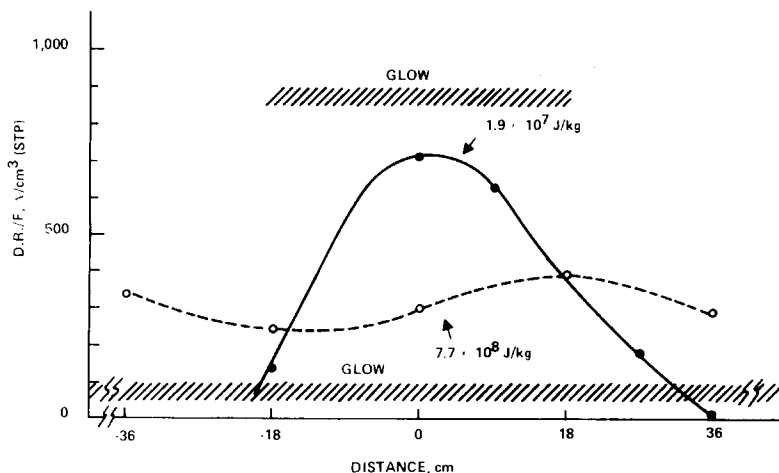


Fig. 1. Distribution of polymer deposition in a reaction time observed with high and low energy input.

have a binding energy of ca. 294 eV. Hydrocarbons (corrected for charging effects) have a binding energy of 284.6 eV. Peaks at binding energy levels of less than 291 eV would represent the presence of crosslinks ( $>CF-$ ,  $>C<$ ) and carbons bonded to other more electronegative substituents, including nitrogen- and oxygen-containing groups. A convenient numerical indicator of the shape of the C1s peak appears to be the ratio of the peak height at 291.5 eV ( $CF_2$ ) to that at 284.6 eV (hydrocarbon). The ratio of peak height at 291.5 eV to that at 284.6 eV is given in the last column of Table I.

Characteristic shapes of C1s peaks are shown in Figures 2 and 3 for the low energy input ( $1.9 \times 10^7$  J/kg) and for the high energy input ( $7.7 \times 10^8$  J/kg) respectively. Figure 2 indicated that the plasma polymer of tetrafluoroethylene formed at the upstream side of the rf coil in the low-energy input discharge contains considerable amounts of  $CF_3$ ,  $CF_2$ , and CF.

TABLE I  
Summary of ESCA Data for Plasma Polymer of Tetrafluoroethylene

Distance, cm	Peak area, (counts · eV) $\times 10^{-4}$				Elemental ratio			Peak Height Ratio (C1s 291.5 eV/ C1s 284.6 eV)
	O1s	F1s	C1s	A12	O/C	F/C	Al/C	
	$F = 5.6 \text{ cm}^3(\text{S.T.P.})/\text{min}, 8 \text{ watts}, 1.9 \times 10^7 \text{ J/kg}$							
-18	0.135	4.01	2.65	0	0.051	1.51	0	1.75
0	0.098	3.71	2.65	0	0.037	1.40	0	1.52
9	0.108	3.78	2.58	0	0.042	1.47	0	1.41
27	0.961	2.18	1.92	0.664	0.50	1.14	0.35	0.261
36	1.33	1.38	1.73	0.913	0.77	0.80	0.53	0.184
	$F = 0.56 \text{ cm}^3(\text{S.T.P.})/\text{min}, 32 \text{ watts}, 7.7 \times 10^8 \text{ J/kg}$							
-36	1.18	1.58	1.41	1.09	0.84	1.12	0.77	0.052
-18	1.16	1.38	1.38	1.29	0.84	1.00	0.94	0.020
0	1.09	1.39	1.49	0.95	0.73	0.94	0.64	0.0098
18	1.29	1.21	1.38	1.24	0.94	0.88	0.90	0.023
36	1.50	0.73	1.57	1.01	0.96	0.46	0.64	0.013

<sup>a</sup> Corrected peak area using photoelectric cross sections relative to C1s.

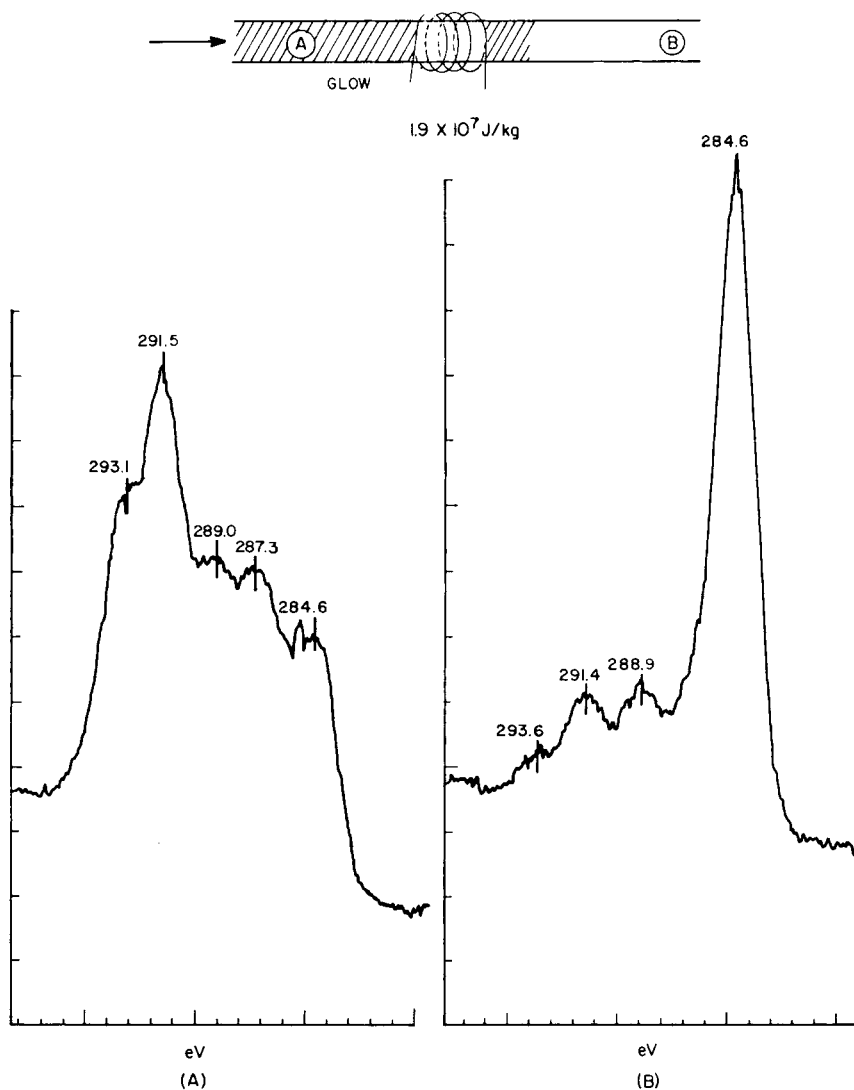


Fig. 2. C1s spectrum of polymer deposits in the low-energy input discharge: (a) polymer deposit before rf coil; (b) polymer deposit after rf coil.

The polymer formed in the downstream side of the rf coil is considerably different from those found in the upstream side; i.e., much smaller peaks for higher binding energy and the peak at 284.6 eV becomes the major peak. When C1s peaks change from the type shown in (A) to the type shown in (B), Al 2s peaks appear in spite of the obvious polymer deposition on the aluminum substrate.

Figure 3 indicates that polymer formed in the high-energy input discharge is similar to type (B) in Figure 2, and the difference between polymers formed before and after the rf coil is very small. In the case of the higher-energy input discharge, Al 2s peaks are always observed (see Table I).

The ratios of F/C based on ESCA peak area shown in Table I are shown in Figure 4 as a function of location of polymer deposition. Figure 4 indicates that the ratio of F/C is highly dependent on the energy input level (i.e., the higher the energy input, the lower the F/C ratio) and decreases as a function of distance from

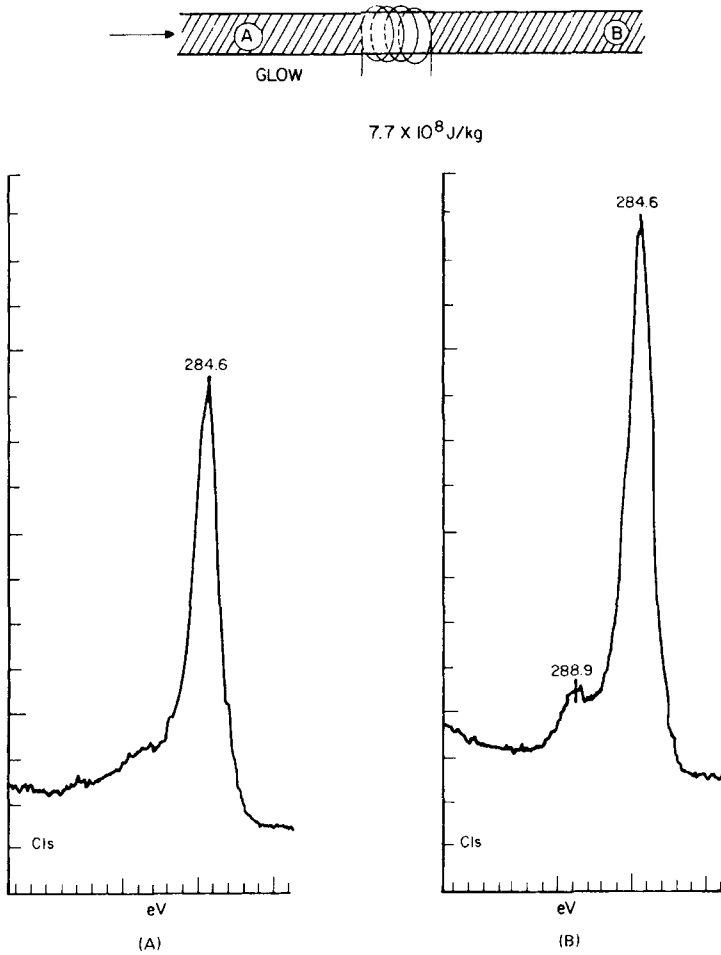


Fig. 3. C1s spectrum of polymer deposition in the high-energy input discharge: (a) polymer deposit before rf coil; (b) polymer deposit after rf coil.

the tip of glow. This loss of fluorine may be related to the high tendency of losing fluorine from fluorocarbon polymers in the plasma environment.

The log of the 291.5/284.6 eV peak height ratio is similarly plotted against location in Figure 5. There is a clear similarity to Figure 4. However, it may be noted that the range of ordinate values for the high  $W/FM$  curve in Figure 5 is clearly separated from that for the low  $W/FM$  curve. In Figure 4, both curves cover nearly the same range of fluorine/carbon ratios. This suggests that the population of  $CF_2$  groups is much greater for all  $1.9 \times 10^7$  J/kg polymers than for the  $7.7 \times 10^8$  J/kg polymers and that in the latter case much of the fluorine observed (see Table I, Figure 4) may be bound to aluminum.

The loss of fluorine in polymers formed in the high-energy input discharge and also in the downstream side of the low-energy input discharge is clearly reflected in the high polar contribution of surface energy as shown in Table II.

These results are in accordance with the previously reported important features of plasma polymerization of perfluorocarbons.<sup>15</sup> Namely, perfluorocarbons are sensitive to plasma condition. The deposition rate, the distribution of

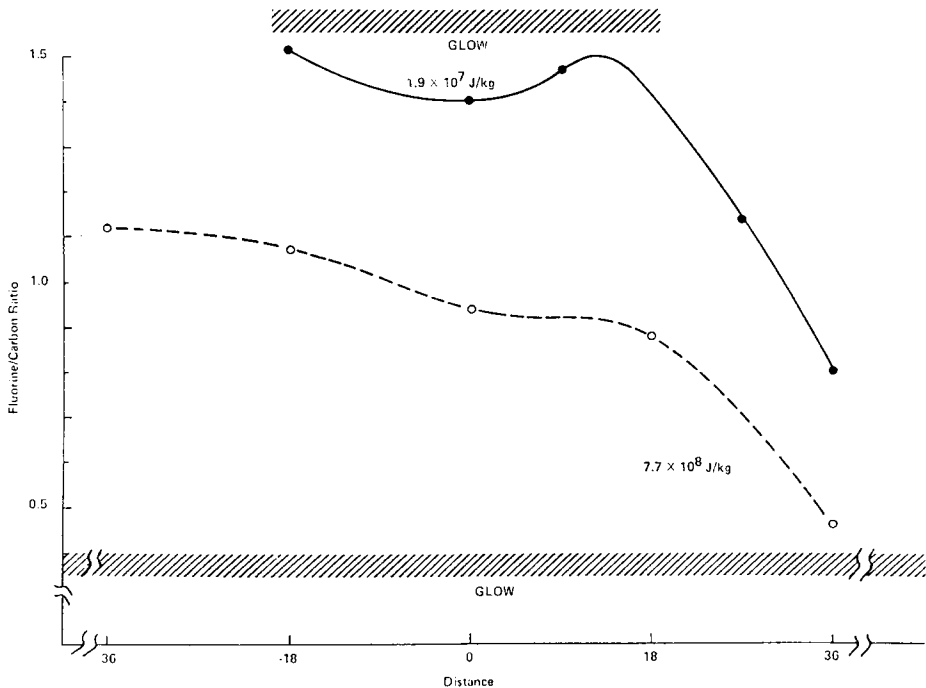


Fig. 4. Change of F/C ratio due to the location of polymer deposition and to energy input level.

TABLE II  
Summary of Surface Energy Data for Plasma Polymer of Tetrafluoroethylene

Distance, cm	$\gamma_s^d$	$\gamma_s^p$	$\gamma_s = \gamma_s^d + \gamma_s^p$
$F = 5.6 \text{ cm}^3 \text{ (S.T.P.)/min, 8 watts, } 1.9 \times 10^7 \text{ J/kg}$			
-18	12.8	2.90	15.7
0	18.9	0.04	18.9
9	19.6	0.09	19.7
27	17.9	0.19	18.1
36	13.5	5.34	18.8
$F = 0.56 \text{ cm}^3 \text{ (S.T.P.)/min, 32 watts, } 7.7 \times 10^8 \text{ J/kg}$			
-36	12.7	2.07	14.8
-18	16.8	2.01	18.8
0	4.03	61.9	65.9
18	13.7	49.3	63.0
36	11.9	40.6	52.5

polymer deposition within a reactor, and the properties of plasma polymers of perfluorocarbons are highly dependent on the energy input level and the design of a reactor. In other words, the values of  $(W/FM)_e$  (necessary to establish glow conditions) and  $(W/FM)_d$  (for the level of energy input where the ablation becomes the predominant process) are not as widely separated as for most monomers. On the other hand, this tendency of the monomer to be sensitive to the energy input level, and the high binding energy shift observed in ESCA C1s peaks of fluorine-containing polymers, make the plasma polymerization of tetrafluoroethylene a unique model for the study of plasma polymerization of organic compounds. This feature will be utilized in the following parts where the different discharge (e.g., capacitive discharge using different frequency power source) will be employed.

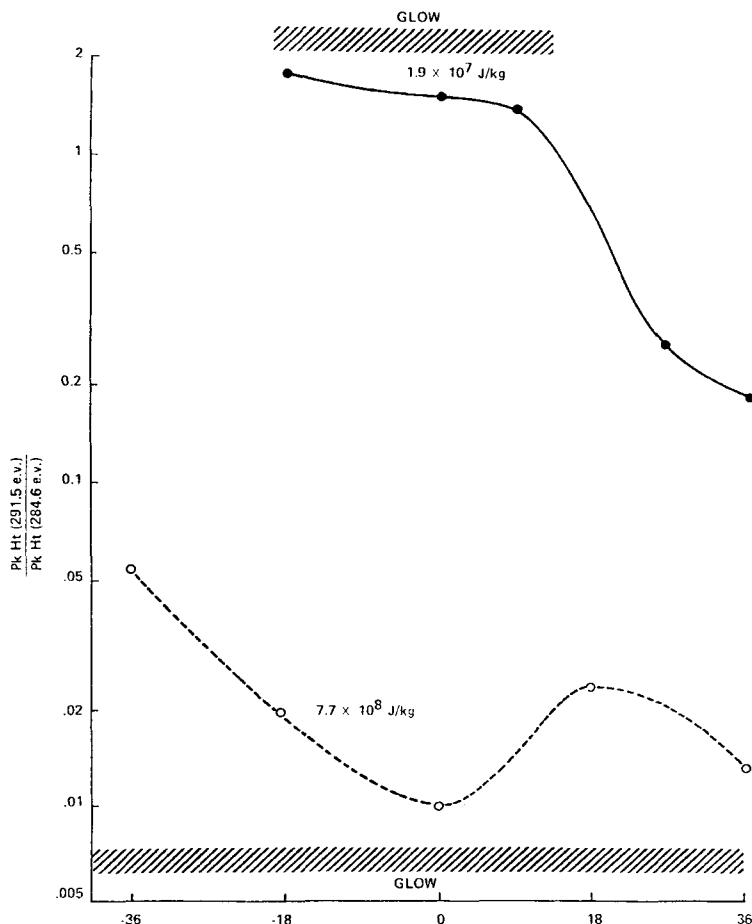


Fig. 5. Change of peak height ratio (C1s 291.5 eV/C1s 284.6 eV) due to the location of polymer deposition and to energy input level. Plot is semilogarithmic.

According to the CAP mechanisms of plasma polymerization,<sup>18</sup> the materials used as the substrate also play an important role in the overall plasma polymerization. This aspect is clearly seen in plasma polymerization of tetrafluoroethylene at high  $W/FM$ , where ablation is significant. The presence of ESCA aluminum peaks with samples which generally have over 100-Å-thick plasma coating seems to reflect CAP mechanisms (i.e., polymerization is competing with ablation process). A separate SEM observation of surfaces indicated that the coating is uniform despite the presence of aluminum. ESCA aluminum peaks are not identical to those for uncoated aluminum foil. It seems, therefore, aluminum is sputtered and some portion redeposits with polymer. The use of aluminum may also cause another artifact of inductive heating of the substrate. However, no obvious effect has been seen within the range of experimental conditions employed in this study.

This study was supported by the National Heart and Lung Institute, NIH, U.S. Department of Health, Education and Welfare, Contract No. NIH-NO1-HV-3-2913. The authors are indebted to Mr. John Guill who prepared the plasma polymer samples. Two of the authors, E.S.B. and C.N.R., are grateful for funding supplied during the period of this study from the National Science Foundation.



## References

1. G. Smolinsky and M. J. Vasile, *Int. J. Mass Spectrom. Ion Phys.*, **12**, 147 (1973).
2. M. J. Vasile and G. Smolinsky, *Int. J. Mass Spectrom. Ion Phys.*, **13**, 381 (1974).
3. H. Kobayashi, A. T. Bell, and M. Shen, *Macromolecules*, **7**, 277 (1974).
4. G. Smolinsky and M. J. Vasile, *Int. J. Mass Spectrom. Ion Phys.*, **16**, 137 (1975).
5. M. J. Vasile and G. Smolinsky, *Int. J. Mass Spectrom. Ion Phys.*, **16**, 179 (1975).
6. G. Smolinsky and M. J. Vasile, *J. Macromol. Sci.-Chem.*, **A10**(3), 473 (1976).
7. G. Smolinsky and M. J. Vasile, *Int. J. Mass Spectrom. Ion Phys.*, **21**, 171 (1976).
8. M. J. Vasile and G. Smolinsky, *Int. J. Mass Spectrom. Ion Phys.*, **21**, 263 (1976).
9. M. J. Vasile and G. Smolinsky, *Int. J. Mass Spectrom. Ion Phys.*, **24**, 11 (1977).
10. G. Smolinsky and M. J. Vasile, *Int. J. Mass Spectrom. Ion Phys.*, **24**, 311 (1977).
11. M. Duval and A. Théorêt, *J. Appl. Polym. Sci.*, **17**, 527 (1973).
12. J. M. Tibbitt, M. Shen, and A. T. Bell, *J. Macromol. Sci.-Chem.*, **A10**(8), 1623 (1976).
13. H. Yasuda and T. Hsu, *J. Polym. Sci., Polym. Chem. Ed.*, **16**, 415 (1978).
14. H. Yasuda and T. Hirotsu, *Rad. Phys. Chem.*, in press.
15. H. Yasuda and T. Hirotsu, *J. Polym. Sci., Polym. Chem. Ed.*, **16**, 743 (1978).
16. H. Yasuda, H. C. Marsh, E. S. Brandt, and C. N. Reilley, *J. Polym. Sci., Polym. Chem. Ed.*, **15**, 991 (1977).
17. P. J. Dynes and D. H. Kaelble, *J. Macromol. Sci.-Chem.*, **A10**, 535 (1976).
18. H. Yasuda and T. Hsu, *Surf. Sci.*, **76**, 232 (1978).

Received October 17, 1977

Revised December 7, 1977